The Field-Emission and Current−Voltage Characteristics of Individual W5O14 Nanowires

ARTICLE *in* THE JOURNAL OF PHYSICAL CHEMISTRY C · MARCH 2008

Impact Factor: 4.77 · DOI: 10.1021/jp8002273

THE JOURNAL OF PHYSICAL CHEMISTRY C LETTERS

2008, *112,* 5250−5253
Published on Web 03/18/2008

The Field-Emission and Current−Voltage Characteristics of Individual W_5O_{14} Nanowires

Marko Žumer,*,† Vincenc Nemanič,† Bojan Zajec,† Mingsheng Wang,‡ Jingyun Wang,‡ Yang Liu,‡ and Lian-Mao Peng‡

"Jožef Stefan" Institute, Jamova 39, 1000 Ljubljana, Slovenia, and Key Laboratory for the Physics and Chemistry of Nanodevices and Department of Electronics, Peking University, Beijing 100871, China

Received: January 10, 2008; In Final Form: March 3, 2008

The field-emission and current−voltage characteristics of individual W_5O_{14} nanowires were studied using a transmission electron microscope and a field-emission microscope. The individual W_5O_{14} nanowires made good ohmic contacts with W and Pt at room temperature and had excellent field-emission properties. The field-emission measurements showed that a current as high as 35 μA can be extracted from a single nanowire. A reduced angular current density of 28.7 $nAsr^{-1}V^{-1}$ was obtained from a W_5O_{14} nanowire with a sharp tip. These results suggest that W_5O_{14}nanowires might be a realistic candidate as the source for a low-energy electron beam.

Introduction

In recent years, a variety of materials have been synthesized in the form of nanowires[1−7,] nanorods,[8−12] nanobelts,[13] and/or nanotubes.[14−16] This has been followed by extensive research on the electrical properties, either for potential applications as the building blocks for nanoelectronics as active components and/or interconnects[17,18] or for the generation of narrow electron beams.[19,20] Research into their size-dependent and low-dimensional physical and chemical properties drew our attention to tungsten suboxides, which have a high aspect ratio and promising physical properties at the nanoscale level. It has been demonstrated that $W_{18}O_{49}$ exhibits excellent field-emission (FE) characteristics[21] and that it can be synthesized in the form of extremely pure and defect-free crystals, as the electrical conductivity of the materials is relatively high.

Motivated by these results, we have studied the field-emission and two-terminal current−voltage properties of mostly pure quasi-one-dimensional tungsten oxide (W_5O_{14}) nanowires (NWs), and have found that these nanowires have all the properties required of a good field emitter.

Experimental Section

Most FE measurements are performed in a transmission electron microscope (TEM), a scanning electron microscope (SEM), or a field-emission microscope (FEM). In a TEM or SEM, the FE of a single NW can be obtained and effects related to the tip structure can be investigated. However, in a real FE device, the reduced angular current density distribution is an additional important characteristic, which is usually studied in a FEM. So, here we combine these methods in two different experimental setups at two locations to get a more complete insight into the following characteristics: the two-terminal current−voltage ($I-V$) dependence, the FE and reduced angular current density of W_5O_{14} nanowires, and the sensitivity of these nanowires to a transfer between systems. All the experiments were performed at room temperature.

In the first experimental setup, the field-emission characterization together with the two-terminal $I-V$ measurements were conducted inside a 200-keV Tecnai G20 TEM equipped with a Nanofactory, a scanning-tunneling-microscope sample holder. The vacuum in the electron microscope was about 10^{-7}mbar. A 0.30 mm Pt wire and an electrochemically etched W tip were used as the electrical leads.

The W_5O_{14} nanowires used in this work were synthesized with a chemical transport reaction using NiI_2 as the growth promoter. The details of the synthesis of this rarely synthesized phase and its characterization have been reported elsewhere.[22] The W_5O_{14} nanowires were assembled onto the Pt wire before the series of experiments by rubbing the Pt wire in the nanowire powder. The W tip was controlled to move in three dimensions by a piezotube with a minimum step of 0.02 nm, while the Pt electrode remained stationary. A maximum of 140 V could be applied between these two electrodes. The W tip was melted in situ inside the TEM into a ball with a clean and smooth surface using resistive heating to improve the electrical contact. To avoid a change in the contact resistance during the experiments, an electron-beam-induced deposition (EBID) of amorphous carbon (a-C) was applied to the W/W_5O_{14} nanowire contact for the FE characterization and additionally to the Pt/ W_5O_{14} nanowire contact for the two-terminal $I-V$ measurements.[23] The a-C layer was built up by the immobilization and decomposition of organic molecules due to complex electron-beam-induced reactions. These molecules originate from the residual atmosphere and are adsorbed to and migrate on the surface of the sample.

Results and Discussion

Figure 1a shows a nanowire firmly fixed to the top of the W tip. The two-terminal *I-V* curve shows that W and Pt form a

* To whom correspondence should be addressed. E-mail: marko.zumer@ijs.si.
† "Jožef Stefan" Institute.
‡ Peking University.

10.1021/jp8002273 CCC: $40.75

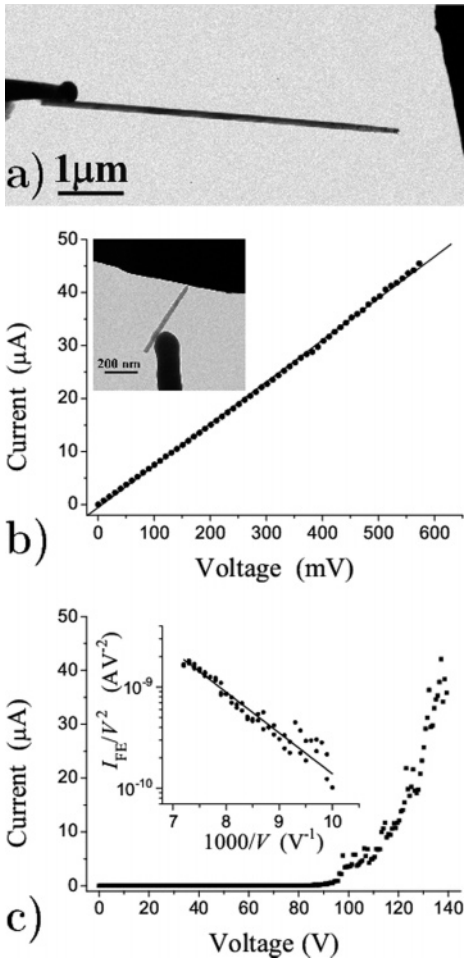

Figure 1. (a) The W_5O_{14}nanowire is firmly fixed to the top of the W tip. ($L = 4.80$ μm, $d = 100$ nm). The distance between the nanowire tip and the anode is 0.87 μm. (b) Typical $I-V$ two-terminal curve shows a good electrical conductivity ($R = 1.27 \times 10^4$ Ω) at room temperature. The thin line shows the corresponding linear fit. The typical measuring setup is shown in the inset. (c) The field emission $I-V$ curve and, shown in the inset, the corresponding Fowler−Nordheim plot.

good ohmic contact at room temperature to the W_5O_{14} nanowire, Figure 1b, which is important for FE materials. A typical estimation for the conductivity σ is 1.4×10^4 Sm^{-1}. The inset of Figure 1b shows the two-terminal measurement setup with the W_5O_{14} nanowire and the W and Pt electrodes. Figure 1c shows that a large FE current can be extracted from the nanowire (~35 μA) before it is discharged. The inset shows the corresponding Fowler−Nordheim curve. The best fit for the measuring points exhibits a fairly linear dependence, which indicates that the FE can be understood as a standard barrier-tunelling mechanism.

To get an additional insight into the characteristics of the W_5O_{14} nanowires, a second experimental setup, a classical FEM with a diode configuration designed for a point-to-plane geometry, was applied. The $I-V$ relationships, the concurrent FEM imaging, and FE current stability ($I-t$), and the reduced angular current density distribution could thus be obtained.

This setup was designed as a part of a miniature ultrahigh vacuum (UHV) system with a high-resolution luminescent screen serving as the anode. A base pressure below 10^{-10} mbar was maintained by a miniature ion-getter pump. The samples were prepared beforehand in the TEM as described in the first experimental setup. A typical aspect ratio (length versus diameter of the NW) of about 50 was chosen for these samples. A final check, which confirmed the presence of a nanowire on

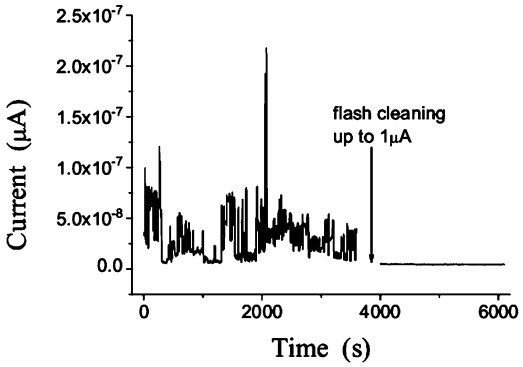

Figure 2. Emission current as a function of time for a single W_5O_{14}-nanowire. The current fluctuation dropped from 63 to 3.5% after flashing at ~1 μA.

the W tip, was performed in an SEM immediately before mounting into the FEM. The miniature UHV system was designed to evaluate one sample at a time. In total, two samples were evaluated, and we present here the results collected from the better sample. The FE measurements were started after an overnight bake-out at 150 °C. First, the onset of the FE current was rather abrupt, but it became stable later, which made it possible to record repeatable $I-V$ diagrams. This priming effect was previously observed on individual inorganic nanowires, and the most probable explanation is either the formation of nanoprotrusions induced by the electric field[24] or an improvement of the ohmic contact to the substrate.[25] The FE current was intentionally limited to below 2 μA during our evaluations, as W_5O_{14} nanowires are prone to segregate (oxide decomposition) at currents higher than 5−10 μA, as was noticed at the first experimental setup (i.e., the TEM).

Prior to emission-current stability ($I-t$) measurements with a constant voltage bias, the sample was flash cleaned by extracting a FE current of about 1 μA for a few tens of seconds to get rid of the loosely bound adsorbate molecules on the surface of the nanowire. This treatment significantly improved the emission−current stability, as the current fluctuation reduced from 63 to 3.5%, **(**Figure 2**)**. This suggests that flash cleaning of the tip is sufficient to maintain the performance after transferring between the two systems (TEM and FEM) located in two laboratories a considerable distance apart.

The emission current of about 5 nA remained stable over the 40 min stability test span, measured at a sampling rate of 3 Hz. The low anode potential involved (625V) significantly reduced the ion sputtering of the emitter surface.

Images of the FE pattern on the luminescent screen were recorded by a professional, color charge-coupled device (CCD) camera (The Imaging Source DFK31F03 with a resolution of 1024 × 768). The brightness of the luminescent screen was well below saturation limits and the exposure time of the CCD camera was adjusted to avoid over-exposure during the image-capturing process.

Observations of the emission patterns showed that its sharp contour clearly expresses the point-like nature of the electron source. The form of the emission pattern could be in most cases described as a single, circular or elliptical spot with the maximum brightness located close to the center, Figure 3a. The analysis of the FE patterns from the CCD images of the luminescent screen allows an elegant and fast determination of the angular current density $dI/d\Omega$ and the reduced angular current density, defined as $(dI/d\Omega)/V$, where V is the extracting voltage. These two quantities are important parameters for electron-optical applications and show that a comparison of

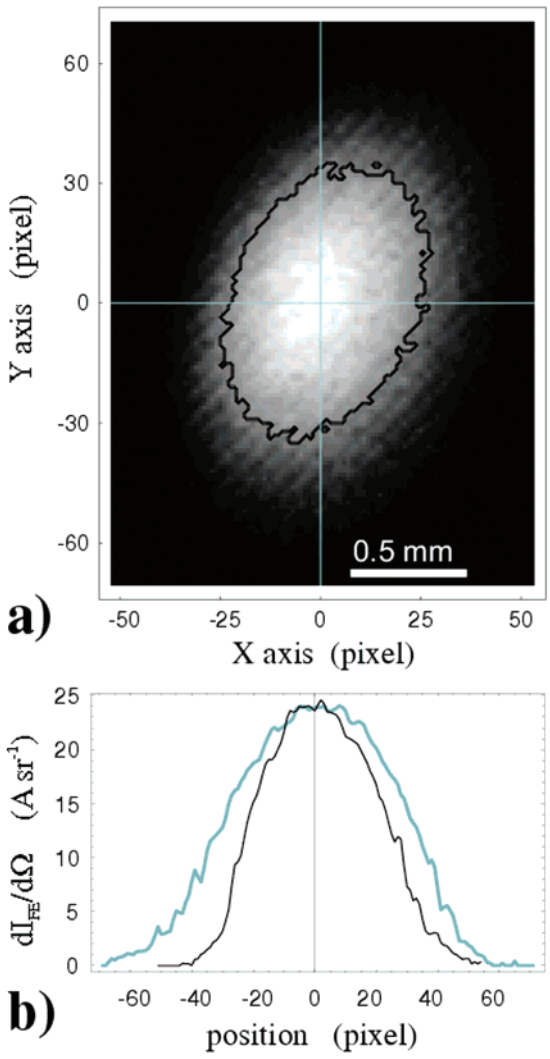

Figure 3. (a) CCD image of a typical FE pattern. The black line contours pixels with a value above one-half of the maximum. The axes origin is set to the average position of the pixels corresponding to the 9 highest values in the image histogram. The average values of these pixels also determine the maximum. (b) Angular current density d*I*/dΩ along the *X* axis (black) and *Y* axis (gray). Besides the central row of pixels, two adjacent rows are included in the calculation to reduce the noise level.

different emitters or the same emitter before and after a certain treatment, such as a bake-out or flash cleaning, has been carried out.

When the luminescent screen and the CCD array are not saturated and the CCD camera operates in the linear mode (gamma = 1), the sum *S* of the red, green and blue values (this is analogous to a conversion to gray scale) of each pixel is linearly proportional to the FE current striking the corresponding part of the screen. The value *S* summed over all the pixels $\sum_j S_j$ is then linearly proportional to the total FE current I_{FE}. The size of a pixel, *a*, is easily obtained using a suitable calibration target. By denoting the distance from the emitter to the screen as *d*, the d*I*/dΩ for a particular pixel *i* is then calculated as

$$\frac{dI_i}{d\Omega} = \frac{d^2 S_i I_{FE}}{a^2 \sum_j S_j} \qquad (1)$$

In our diode configuration, the distance *d* was fixed to 6 mm and the side of 1 pixel was 0.017 mm; hence, we could determine the FE current being emitted into a solid angle of only 8.03×10^{-6} sr. The FE current and the corresponding FE patterns were recorded after various treatments and at various extracting voltages. The highest value of the angular current density reached 25.1 μAsr^{-1} (at $V = 875$ V and $I_{FE} = 0.58$ μA); however, this value originates from the pixel with the highest S_i value, which might not be representative. The same image was therefore smoothed, with the S_i values corresponding to the same 4×4 pixel frame set to their average value. The highest obtained value with the smoothing procedure was then 24.0 μAsr^{-1}. It is clear that the two values are almost equal. The reason lies in the smooth and broad peaked d*I*/dΩ distribution (Figure 3b). The angular spread of the emitted electrons amounts to 9°, measured at the full-width-half-maximum of the d*I*/dΩ distribution.

The best value for the reduced angular current density was also obtained in the same measurement described above; it reached 28.7 $nAsr^{-1}V^{-1}$ in our evaluations of a single sample, which is comparable to the data given by de Jonge[26] for multiwalled carbon nanotubes (~30 $nAsr^{-1}V^{-1}$ as an average for the total of seven samples) and almost an order of magnitude higher than 3.6 $nAsr^{-1}V^{-1}$, which was measured for a W supertip.[27] These results suggest that W_5O_{14} nanowires are promising candidates for replacing existing sources for low-energy electron beams.

The determination of the angular current density and the further reduced angular current density using the above-described method gives the entire distribution of d*I*/dΩ with a single, simple measurement that takes only the few seconds needed to get a CCD image. The details of the distribution of d*I*/dΩ are determined solely by the magnification of the diode setup and the CCD camera's resolution.

Conclusions

We have shown that W_5O_{14} nanowires have all the required properties to be used as a good field emitter, including a relatively high maximum emission current and good emission stability, a high reduced angular current density, and a good ohmic contact with noble metals at room temperature. These characteristics make W_5O_{14} nanowires very promising candidate materials for a point-electron source.

Acknowledgment. The authors would like to thank M. Remskar and her group for the samples of W_5O_{14} nanowires. This work was supported by the Ministry of Science and Technology of China (6-11, 2006AA03Z350), the National Science Foundation of China (Grants 90406024, 10434010, and 90606026), and the Slovenian Research Agency (BI−CN/06-07/11 and Grant J2-9313).

References and Notes

(1) Ma, D. D. D.; Lee, C. S.; Au, F. C. K.; Tong, S. Y.; Lee, S. T. *Science* **2003**, *299*, 1874.
(2) Wang, Y. D.; Zang, K. Y.; Chua, S. J.; Fonstad, C. G. *Appl. Phys. Lett.* **2006**, *89*, 263116.
(3) Qiu, Y. F.; Liu, D. F.; Yang, J. H.; Yang, S. H. *Adv. Mater.* **2006**, *18*, 2604.
(4) Deng, Z. T.; Tang, F. Q.; Chen, D.; Meng, X. W.; Cao, L.; Zou, B. *J. Phys. Chem. B* **2006**, *110*, 18225.
(5) Xiao, Z. D.; Zhang, L. D.; Tian, X. K.; Fang, X. S. *Nanotechnology* **2005**, *16*, 2647.
(6) Zhou, J.; Xu, N. S.; Deng, S. Z.; Chen, J.; She, J. C. *Chem. Phys. Lett.* **2003**, *382*, 443.
(7) Zhu, Y. W.; Yu, T.; Cheong, F. C.; Xu, X. J.; Lim, C. T.; Tan, V. B. C.; Thong, J. T. L.; Sow, C. H. *Nanotechnology* **2005**, *16*, 88.
(8) Cao, M.; Hu, C.; Peng, G.; Qi, Y.; Wang, E. *J. Am. Chem. Soc.* **2003**, *125*, 4982.

(9) Kwon, S. J.; Park, J. H.; Park, J. G. *J. Electroceram.* **2006**, *17*, 455.
(10) Zhao, Y. M.; Li, Y. H.; Ma, R. Z.; Roe, M. J.; McCartney, D. G.; Zhu, Y. Q. *Small* **2006**, *2*, 422.
(11) Chen, R. S.; Korotcov, A.; Huang, Y. S.; Tsai, D. S. *Nanotechnology* **2006**, *17*, R67.
(12) Pavasupree, S.; Suzuki, Y.; Kitiyan, A.; Pivsa-Art, S.; Yoshikawa, S. *J. Solid State Chem.* **2005**, *178*, 2152.
(13) Pan, Z. W.; Dai, Z. R.; Wang, Z. L. *Science* **2001**, *291*, 1947.
(14) Li, F.; Wang, X. H.; Shao, C. L.; Tan, R. X.; Liu, Y. C. *Mater. Lett.* **2007**, *61*, 1328.
(15) Wu, M. S.; Lee, J. T.; Wang, Y. Y.; Wan, C. C. *J. Phys. Chem. B* **2004**, *108*, 16331.
(16) Goldberger, J.; Hee, R. R.; Zhang, Y. F.; Lee, S. W.; Yan, H. Q.; Choi, H. J.; Yang, P. D. *Nature* **2003**, *422*, 599.
(17) Lu, W.; Lieber, C. M. *J. Phys. D: Appl. Phys.* **2006**, *39*, R387.
(18) Nguyen, P.; Ng, H. T.; Yamada, T.; Smith, M. K.; Li, J.; Han, J.; Meyyappan, M. *Nano Lett.* **2004**, *4*, 651.
(19) Dong, L.; Jiao, J.; Tuggle, D. W.; Petty, J. M.; Elliff, S. A.; Coulter, M. *Appl. Phys. Lett.* **2003**, *82*, 1096.
(20) Zumer, M.; Nemanic, V.; Zajec, B.; Remskar, M.; Mrzel, A.; Mihalovic, D. *Appl. Phys. Lett.* **2004**, *84*, 3615.
(21) Li, Y. B.; Bando, Y.; Goldberg, D. *Adv. Mater.* **2003**, *15*, 1294.
(22) Remskar, M.; Kovac, J.; Virsek, M.; Mrak, M.; Jesih, A.; Seabaugh, A. *Adv. Func. Mater.* **2007**, *17*, 1974.
(23) Wang, M. S.; Wang, J. Y.; Chen, Q.; Peng, L. M. *Adv. Func. Mater.* **2005**, *15*, 1825.
(24) Zumer, M.; Nemanic, V.; Zajec, B.; Remskar, M.; Ploscaru, M.; Vengust, D.; Mrzel, A.; Mihailovic, D. *Nanotechnology* **2005**, *16*, 1619.
(25) Chen, Q.; Wang, S.; Peng, L. M. *Nanotechnology* **2006**, *17*, 1087.
(26) de Jonge, N. *J. Appl. Phys.* **2004**, *95*, 673.
(27) Knoblauch, A.; Wilbertz, Ch.; Miller, Th.; Kalbitzer, S. *J. Phys. D: Appl. Phys.* **1996**, *29*, 470.